Published online 21 June 2011

Nucleic Acids Research, 2011, Vol. 39, No. 16 ***e110***
doi:10.1093/nar/gkr504

Rational, modular adaptation of enzyme-free DNA circuits to multiple detection methods

Bingling Li, Andrew D. Ellington and Xi Chen*

Institute for Cellular and Molecular Biology, Center for Systems and Synthetic Biology, Department of Chemistry and Biochemistry, University of Texas at Austin, Austin, TX 78712, USA

Received January 28, 2011; Revised June 2, 2011; Accepted June 3, 2011

ABSTRACT

Signal amplification is a key component of molecular detection. Enzyme-free signal amplification is especially appealing for the development of low-cost, point-of-care diagnostics. It has been previously shown that enzyme-free DNA circuits with signal-amplification capacity can be designed using a mechanism called 'catalyzed hairpin assembly'. However, it is unclear whether the efficiency and modularity of such circuits is suitable for multiple analytical applications. We have therefore designed and characterized a simplified DNA circuit based on catalyzed hairpin assembly, and applied it to multiple different analytical formats, including fluorescent, colorimetric, and electrochemical and signaling. By optimizing the design of previous hairpin-based catalytic assemblies we found that our circuit has almost zero background and a high catalytic efficiency, with a k_{cat} value above 1 min^{-1}. The inherent modularity of the circuit allowed us to readily adapt our circuit to detect both RNA and small molecule analytes. Overall, these data demonstrate that catalyzed hairpin assembly is suitable for analyte detection and signal amplification in a 'plug-and-play' fashion.

INTRODUCTION

Nucleic acids are frequently used to amplify signals during the detection of both nucleic acids and non-nucleic acid analytes including proteins and small molecules. In applications such as immuno-PCR (1,2), target-dependent rolling circle amplification (3,4), and the proximity ligation assay (5,6), nucleic acids frequently act as captured or created templates for amplification. It is also possible to rely on ribozymes, rather than protein enzymes, for amplification. For example, RNA-cleaving deoxyribozymes (7,8) and RNA-ligating ribozymes (9,10) have been used to construct autocatalytic or cross-catalytic circuits for exponential signal amplification in the detection of nucleic acid and/or small molecule analytes. While nucleic acid-alone amplification schemes have the advantage of operating under conditions that might otherwise inhibit proteins, they currently have the disadvantage of requiring a great deal of engineering for adaptation to any given analyte. For example, directed evolution of the Bartel Class I ligase was necessary in order to adapt it to detecting a particular mRNA sequence (11).

Recent advances in the field of molecular programming (12–15) have yielded DNA circuits in which the simple rules governing nucleic acid hybridization can be adapted to signal-amplification. The hybridization chain reaction (HCR) (16,17), entropy-driven catalysis (18), and catalyzed hairpin assembly (19) rely only on hybridization and strand-exchange reactions in order to achieve amplification.

Some hybridization-based, nucleic-acid-alone circuits have been adapted to analytical applications. For example, the Pierce group has successfully used the hybridization chain reaction for multiplexed imaging of endogenous mRNA in fixed zebrafish embryos (17). The application of HCR and entropy-driven catalysis in assisting *in vitro* nucleic acid detection has also been reported (20–22). Building on these results, we believe that there now exists an even greater potential to adapt catalyzed hairpin assembly (19) to support even more robust analytical applications.

A key feature of nucleic acid circuits for molecular amplification is that they do not require perishable protein enzymes. Although some enzymes can be stored for a relatively long period of time in a dry or semi-dry state, all oligonucleotides are amenable to such storage. Moreover, nucleic acid circuits are inherently modular and scalable, requiring only the design of base-pairing between strands. However, within this broad context there are several practical analytical features that should be achieved. First, the uncatalyzed reaction must be sufficiently slow to ensure low background. Second, the turnover of substrates must

*To whom correspondence should be addressed. Tel: +512 471 6445; Fax: +512 471 7014; Email: xichen@mail.utexas.edu

be fast enough so that a high level of signal amplification can be achieved in a relatively short period of time. Third, it should be possible to adapt the catalyst to detect various analytes. And finally, the product of the catalysis should be easily detectable by common detection modalities, such as fluorescence, colorimetric, or electrochemical detection.

In this work, we designed a simplified DNA circuit based on catalyzed hairpin assembly. Kinetic characterization of this circuit showed that the uncatalyzed background assembly was undetectable ($<0.5\,M^{-1}s^{-1}$). This result is particularly noteworthy since uncatalyzed background reactions have been a major challenge in the design of DNA circuits for analytical applications. In particular, the original hairpin assembly circuit (19) had an uncatalyzed rate constant as high as $\sim 100\,M^{-1}s^{-1}$. In addition, our circuit was very efficient and steady-state analysis showed that the turnover rate of the catalyst was $>1\,min^{-1}$, yielding 50- to 100-fold signal amplification within a few hours. Finally, the modularity of the DNA circuit allowed its adaptation to detect various analytes. For example, we engineered a molecular beacon (23,24) to act as a signal transducer for virtually any nucleic acid sequence, and showed that similar aptamer beacon (25–27) transducers allowed the detection of non-nucleic acid analytes. The circuit's modularity also allowed the output to be readily switched between fluorescence, electrochemical (28,29), or colorimetric readouts (30–33). Overall, these data suggest a paradigm for circuit-based molecular detection in which target recognition, signal processing, amplification, and transduction can be integrated via modular components.

MATERIALS AND METHODS

Chemicals, oligonucleotides and oligonucleotide complexes

All chemicals were of analytical grade and were purchased from Sigma-Aldrich (MO, USA) unless otherwise indicated. The methylene-blue labeled oligonucleotide (mH1H2-MB) was ordered from Biosearch Technologies (Novato, CA, USA). All other nucleotides were ordered from Integrated DNA Technology (IDT, Coralville, IA, USA). Oligonucleotide sequences are summarized in Supplementary Table S1. H1-E was prepared by ligating 10 nmol of H1.a and 10 nmol of mH1H2-MB with 16 U of T4 DNA ligase (Invitrogen, Carlsbad, CA, USA) in a 160-μl reaction in 1× T4 ligase buffer (Invitrogen) at room temperature overnight. H1, H1-E, H2, hpC1, $siEGFP_{AS}$, AptC1, and AptInh were purified via denaturing PAGE (7 M Urea, 1× TBE). C1, C1mut, Dz, DzInh and mH1H2 were simply ethanol-precipitated to remove salts that might interfere with 260 nm absorption readings. All DNA strands were stored in 1× TE (pH 7.5) at 1–100 μM concentrations. Diluted C1, mutC1, and $siEGFP_{AS}$ stocks (1 pM to 100 nM) were stored in 1× TE (pH 7.5) supplemented with 1 μM $(dT)_{21}$ to prevent loss due to adsorption to plastic. Nucleosides were purchased from Alfa Aesar (Ward Hill, MA, USA).

Estimation of rate constants of circuits previously designed by Yin et al.

In Figure 3c of (19), the trace 'A+B' showed that when 20 nM hairpin A and 20 nM hairpin B were mixed in the absence of catalyst, 3.5% of A (0.7 nM) was hybridized with B after 5 h of reaction. Assuming linearity of the reaction, this corresponds to a rate of (0.7/5 =) $0.14\,nM\ h^{-1}$. The second order rate constant can be estimated to be (0.14/20/20 =) $3.5 \times 10^{-4}\,nM^{-1}h^{-1}$, or $97\,M^{-1}s^{-1}$. Although the accuracy of this estimation might be affected by a mixed population of both fast-reacting and slow-reacting hairpins (see Discussion section), we believe it is roughly accurate.

Real-time fluorescence measurements

An amount of 10 μM stock of RepF:RepQ complex was prepared by annealing 10 μM RepF and 20 μM RepQ in 1× TNaK buffer (20 mM Tris, pH 7.5; 140 mM NaCl; 5 mM KCl). An excess of RepQ ensures efficient quenching of RepF but does not interfere with the readout of H1:H2. All kinetic measurements were carried out at 37°C. Immediately before experiments, H1 and H2 were separately refolded in 1× TNaK buffer. This and other refolding reactions involved heating to 90°C for 1 min followed by slowly decreasing the temperature to 23°C at a rate of $0.1°C\ s^{-1}$. All reagents were prepared in 1× TNaK buffer and were pre-warmed to 37° C for 15–30 min before mixing. The reactions were started by the addition of H1. Reaction mixtures (18 μl aliquots) were added to different wells of a 384-well plate, which was immediately transferred to a TECAN Safire plate reader for fluorescence measurements. With our setting, roughly 67 Raw Fluorescence Units correspond to 1 nM unquenched RepF, which in turn corresponds to 1 nM H1:H2.

For the detection of $siEGFP_{AS}$, different concentrations of $siEGFP_{AS}$ were annealed with a constant concentration of hpC1 (final concentration 5 nM) before the addition of other components of the circuit. For the detection of adenosine, AptC1 and AptInh were annealed at 8× final concentration in 1× TNaK, and then mixed with equal volumes of adenosine (or other nucleosides) at 4× final concentration in 1× TNaK for 2 h at 37°C. Some 5 μl of this mixture was mixed with H1, H2 and RepF:RepQ in a total volume of 20 μl (each component at 1× final concentration).

Conjugation of thiol-labeled oligonucleotide S to the Au electrode

The Au electrode (1.2 mm in diameter) was polished with 1.0, 0.3 and 0.05 μm α-Al_2O_3; washed ultrasonically with pure water three times; and then electrochemically cleaned in 0.1 M H_2SO_4 by potential scanning between 0 and 1.6 V until a reproducible cyclic voltammogram was obtained. The electrode was then sonicated and rinsed with copious amount of pure water, and blown dry with nitrogen.

Before use, the thiol-labeled oligonucleotide **S** was treated with 6.7 mM Tris(2-chloroethyl) phosphate (TCEP) in DP buffer (20 mM Tris–HCl, pH 7.4; 100 mM NaCl; 5 mM $MgCl_2$) for 2 h at 28°C. The Au-**S**

conjugation was performed by placing 20 µl of the 2 µM **S** in DP buffer on the Au electrode. The electrode was capped with a 1.5 ml Eppendorf tube to protect the solution from evaporation. After 16 h of conjugation at room temperature, the electrode was rinsed with pure water several times. Then the **S**-conjugated Au electrode was treated with 1 mM 6-mercapto-1-hexanol (MCH) in DP buffer and kept at room temperature for 1 h, followed by rinsing with pure water.

Detection of methylene blue with S-labeled Au electrode

The catalyzed hairpin assembly reaction was allowed to proceed for 1 h at 37°C. Reaction mixtures (or mH1H2-E solution; 15 µl) were placed on the S/MCH-modified Au electrode, and incubated at 37°C for another 1.5 h. Electrodes were then rinsed with DP buffer at 37°C and square wave voltammetry (SWV) was used to detect the MB near the surface of the electrode. SWV was performed on a DY-2000 Series Multichannel Potentiostat (Digi-Ivy, Inc. Austin, TX, USA) using a conventional three-electrode electrochemical cell with an Ag-AgCl (1 M KCl) electrode (CH Instruments, Austin, TX, USA) as the reference electrode, a Pt coil as the counter electrode, and an Au disk (1.2 mm in diameter) as the working electrode. All the electrochemical measurements were carried out at room temperature. SWV measurements were performed in DP buffer under an oscillatory potential between −0.5 and 0 V, with a frequency of 50 Hz.

Detection of assembled H1:H2 via colorimetric readout

An 8 µM stock of Dz:DzInh complex was prepared by annealing 8 µM Dz and 16 µM DzInh. An excess of DzInh ensures efficient inhibition of Dz but does not interfere with the readout of H1:H2.

The catalyzed hairpin assembly reactions were set up as was described for fluorescence measurements, except RepF:RepQ was not included. In these assembly reactions, the concentrations of H1 and H2 were 600 and 900 nM, respectively. The assembly reactions were incubated at 37°C for 4 h. Then 35 µl of the assembly reaction was mixed with 2.5 µl of 8 µM Dz:DzInh complex and 2.5 µl of 20 µM hemin (in DP buffer supplemented with 0.1% Triton-X100) and incubated for another 2 h at 37°C. To develop color, 36 µl of this mixture was mixed with 4 µl of substrate solution (38 mM ABTS and 20 mM H_2O_2). The 20 µl final mixtures were transferred to different wells of a 384-well plate. The absorption at 410 nm was measured using a Synergy-HT plate reader (Bio-TEK, Winooski, VT, USA). After ~15 min of data collection the plate was removed from the plate reader and a picture of the plate was also taken.

RESULTS

Designing a catalyzed hairpin assembly

The general principle of catalyzed hairpin assembly was introduced in the seminal work by Pierce, Yin, and co-workers (19). One implication of this work is that for any unstructured ssDNA, a pair of hairpins can be designed so that the two hairpins do not initially interact with each other but can catalytically form a duplex in the presence of a ssDNA input. We designed a simple amplification circuit based on this model, shown in Figure 1. As in earlier approaches, we describe the sequence of DNA molecules in terms of numbered domains, each of which represents a short fragment (usually <12 nt) of DNA sequence. Complementarity between numbered domains is denoted by an asterisk. Hairpins H1 and H2 can potentially hybridize to form a H1:H2 duplex, since H1 contains a segment that is complementary to a segment of hairpin H2 (see the H1:H2 duplex in Figure 1). However the spontaneous hybridization of the two hairpins is kinetically hindered by occluding complementary regions within intramolecular hairpin secondary structures. Domain *1** of an unstructured DNA input, C1, serves as a 'toehold' to initiate interactions with domain *1* of H1. Branch migration then opens hairpin H1 and forms a C1:H1 intermediate (Figure 1, reaction *a*). In the C1:H1 intermediate, domain *3** of H1 is no longer occluded and can bind to domain *3* of H2, again initiating a branch migration reaction to form a H1:H2:C1 complex (Figure 1, reaction *b*). This complex is inherently unstable, and C1 dissociates from the H1:H2 complex, completing the reaction and allowing C1 to act as a catalyst to trigger the hybridization of additional pairs of H1 and H2 hairpins. The overall reaction is at least partially driven by the enthalpy decrease resulting from the formation of more base pairs.

While the original circuit (19) was viable, it was not suitable for analytical applications, because of high background reactivity in the absence of input. In order to improve the circuit, we attempted to optimize the design of the individual components at two levels: domain organization and sequence.

We first simplified the hairpin designs by removing unnecessary domains. In the original circuits (19), the hairpin substrates usually contained from 10 to 13 domains. Among these domains, only four to five were necessary to dictate the progression of reaction, while the rest were 'clamp' domains designed to reduce uncatalyzed (background) reactions. Paradoxically, a fast, uncatalyzed reaction ($\sim 100\,M^{-1}s^{-1}$) was still observed for the original circuit, which led us to question the effectiveness of these 'clamp' domains. Therefore, we removed these domains and only kept those domains that were necessary to dictate the progression of the reaction. Our domain organization also differed from the original circuit (19). For example, the loop of H1 (domain *4*) does not contain sequences that are complementary to the overhang (domain *1*), which might help prevent unwanted H1 dimerization.

The lengths of the domains were chosen based on kinetic and thermodynamic considerations. In general, toehold binding should be strong enough to efficiently initiate strand displacement (34) and weak enough to spontaneously dissociate and regenerate the catalyst. Binding should also be poised to prevent unwanted DNA hybridization (e.g. a stable interaction between domain 3* of C1 and domain 3 of H2). By estimating

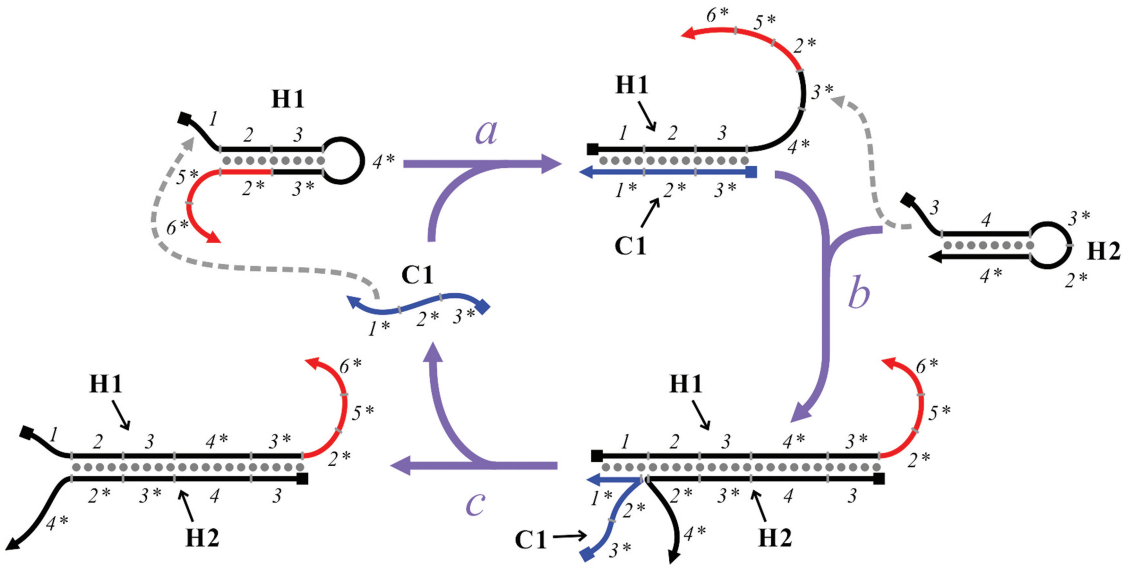

Figure 1. Scheme of catalyzed hairpin assembly. The ssDNA C1 catalyzes the hybridization of hairpins H1 and H2 through a series of toehold-mediated strand displacement reactions (*a*, *b* and *c*). Squares and arrows drawn on DNA strands represent 5′ termini and 3′ termini, respectively. Base-pairing is shown by gray, filled circles. Toehold binding is shown by dotted gray lines with arrows. Domains are named by numbers and complementarity is denoted by asterisks (see text). Junctions between domains are shown as short gray dashes. The segment of H1 that can trigger downstream sensors is shown in red.

the stability of DNA hybridization in the chosen buffer (see 'Materials and Methods' and Discussion sections), we eventually chose 8 nt as the length the of domains *1–3*, *5* and *6*. Since H2 has two mutually exclusive foldings (Figure 2a), we chose 11 nt as the length of domain *4* so that the correct folding would be greatly favored.

The sequence design process is summarized in Figure 2b. The sequence of C1 was chosen within the constraints of avoiding secondary structure and maintaining a GC content of 50% for each domain. This fixed the sequences of domains *1*, *2* and *3*, and left domains *4*, *5* and *6* to be designed. In order to avoid alternative foldings, the NUPACK package (35) was used to design the sequence of domains *4**, *5** and *6** in H1, which in turn defined the sequence of H2. The expected correct folding of H2 was also verified using NUPACK.

Characterization of assembly kinetics

To monitor the assembly of H1 and H2 in real time, we designed a fluorescent reporter by hybridizing a FAM-labeled strand (RepF) and an Iowa Black FQ-labeled strand (RepQ; Figure 3a). Hybridization of these two strands did indeed result in efficient quenching. The domain *2** of H1 in the H1:H2 duplex can bind the domain *2* of RepF in the RepF:RepQ complex and initiate the branch migration reaction to displace RepQ, leading to an increase in fluorescent signal. Since the domain *2** of H1 alone is occluded, H1 alone should not interact with the RepF:RepQ complex.

Using these fluorescent reporter constructs, it can be observed that in the presence 5 nM C1, 50–200 nM H1, and 200 nM H2, the two hairpins rapidly form a duplex (Figure 3b). The reactions approached completion

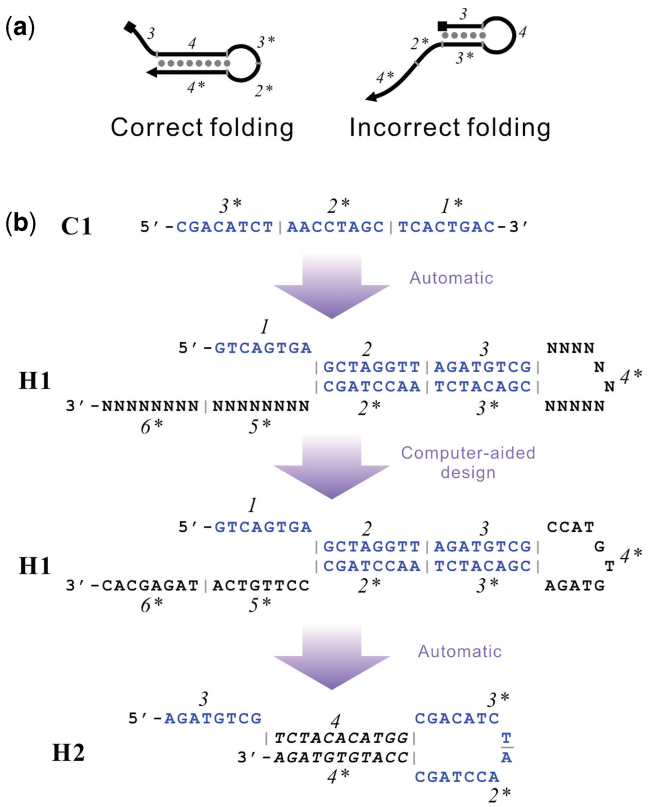

Figure 2. Design of hairpins for catalyzed hairpin assembly. (**a**) The two possible conformations of **H2**. (**b**) Process of sequence design. The sequence of C1 was arbitrarily chosen. Domains whose sequence was defined by the sequence of C1 are shown in blue. New domains whose sequence was designed by NUPACK are shown in black.

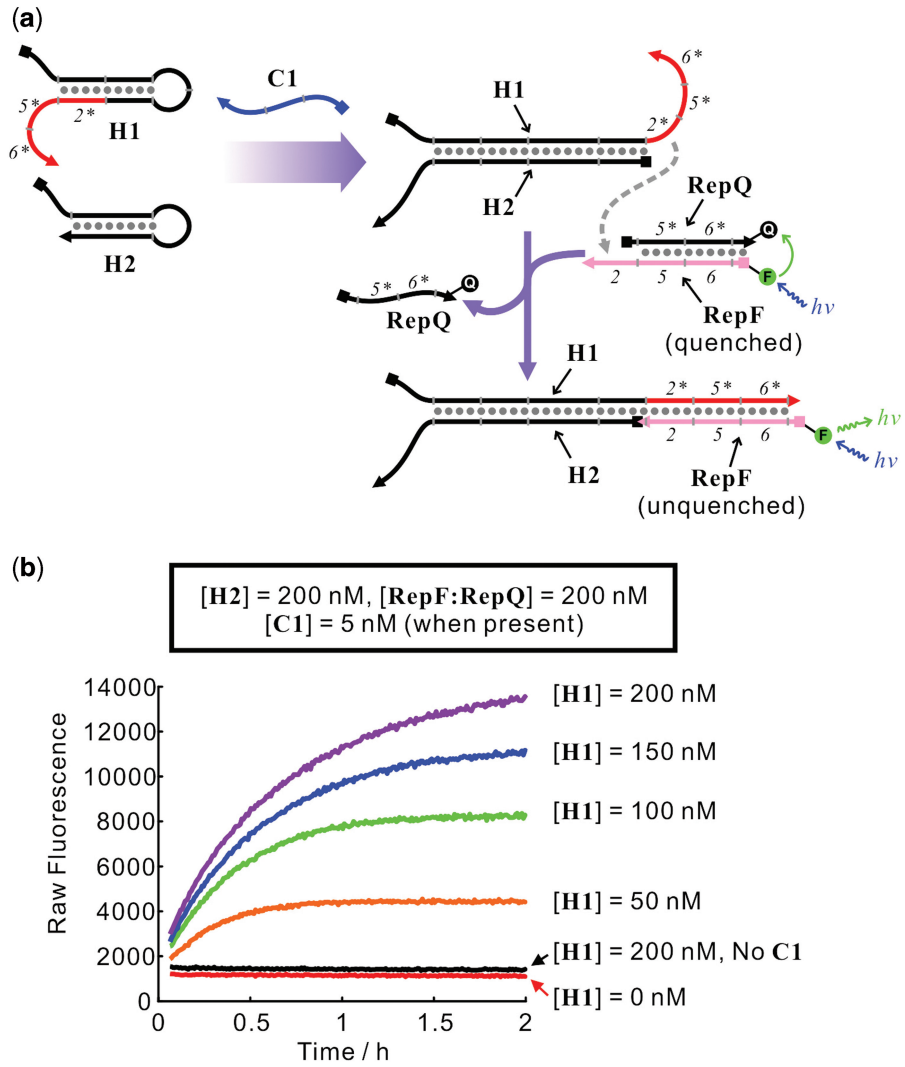

Figure 3. Fluorescent reporter designed to monitor the kinetics of H1:H2 hybridization in real time. (**a**) Design of the fluorescent reporter. The reporter is a duplex consisting of a FAM-labeled strand RepF and an IowaBlack FQ-labeled strand RepQ. Hybridization of H1 and H2 exposes the domain *2** of H1, which leads to the toehold-mediated displacement of RepQ and an increase in fluorescent signal. (**b**) Real-time kinetics of **H1:H2** assembly. The concentration of each species is shown in the panel. The concentrations of species common to all reactions are listed in the inset at the top of the panel.

within 2 h. In contrast, in the absence of C1 no H1:H2 hybridization could be observed (Figure 3b, black line) even with prolonged incubation (up to 15 h, data not shown). Considering the sensitivity of this assay (2 nM H1:H2 should be readily detectable), the second-order rate constant of uncatalyzed reaction can be estimated to be $<0.5\,M^{-1}s^{-1}$, which is at least 200-fold slower than the original circuit (19).

To gain a more quantitative understanding of the efficiency of catalysis, we systematically varied the concentration of H1 and H2 and recorded the initial reaction rates v (Figure 4a). By fitting the dependence of initial rates on substrate concentrations (Figure 4b) with the equation:

$$v = \frac{k_{cat}[C1][H1][H2]}{K_{H2}K_{IH1}+K_{H2}[H1]+K_{H1}[H2]+[H1][H2]}$$

k_{cat} was found to be $1.6 \pm 0.3\,min^{-1}$.

Although other constants in the equation could not be accurately determined, it can be semi-quantitatively estimated that in the presence of 50–400 nM H1 and 100–400 nM H2, the observed turnover rate (v/[C1]) was with the range of $0.3–0.9\,min^{-1}$ (Figure 4b). Such a turnover rate implicates that 20–50 molecules of product (H1:H2 complex) can be produced per molecule of catalyst (C1) per hour. In other words, the signal can potentially be amplified by 20- to 50-fold per hour, suggesting that non-enzymatic DNA circuitry may be useful for sequence detection in many analytical applications.

Modular detection of differing inputs

In order to demonstrate the utility of this amplification method for analytical applications, we first attempted to adapt the system to multiple inputs. The system

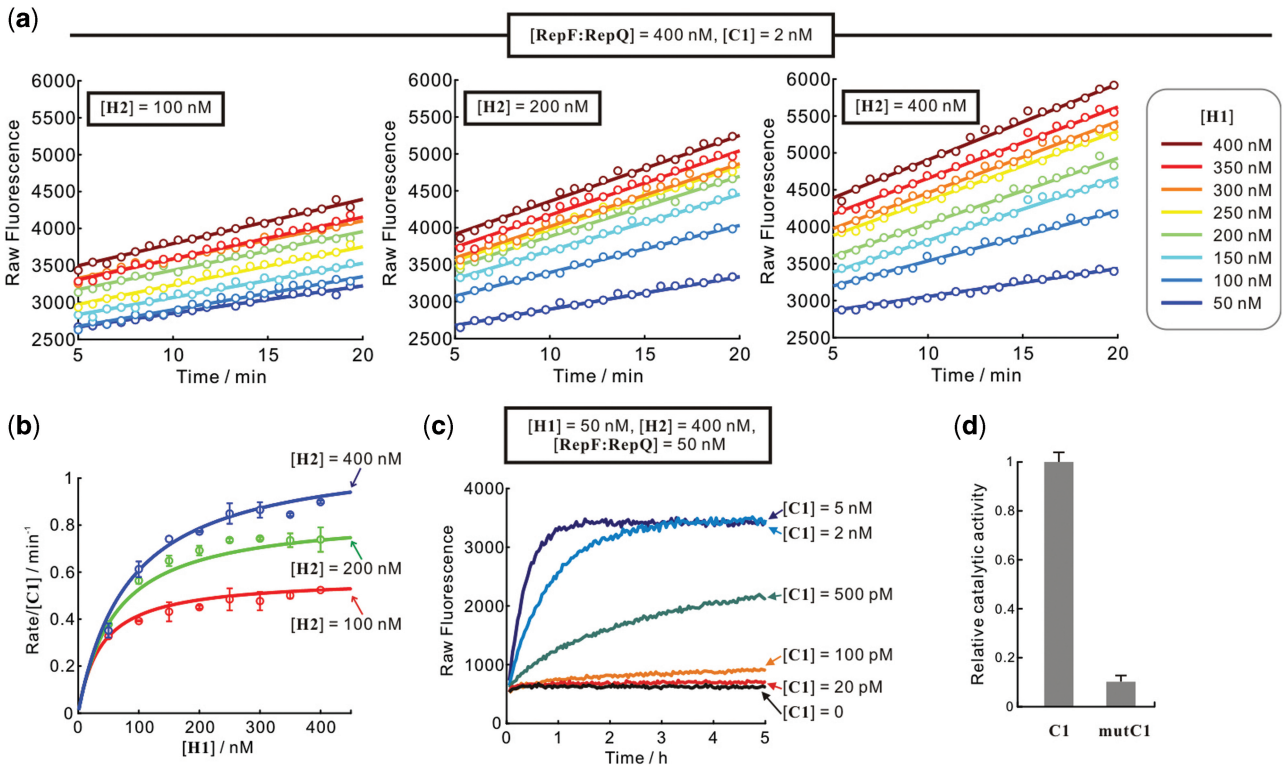

Figure 4. Steady-state kinetics of H1:H2 hybridization and the sensitivity of the circuit. (**a**) Initial kinetics of H1:H2 hybridization when the concentration of H1 and H2 were systematically varied. The concentrations of H2 are shown in the inset of each plot. The concentrations of H1 are color-coded as shown in the legend box to the right. The concentrations of species common to all reactions are listed in the inset at the top of the panel. Circles and lines represent raw data and linear regressions, respectively. (**b**) The dependence of initial rate on the concentration of H1 and H2. Two independent readings were carried out for each combination of H1 and H2 [one is shown in (**a**)], and the standard deviations of the obtained rates are shown as error bars. (**c**) The sensitivity of the circuits. Different concentrations of C1 were added to H1, H2, RepF:RepQ and the raw fluorescence values produced are shown. (**d**) Sequence specificity of the circuit. MutC1, which varies from **C1** by a C-to-A change at the second position (from the 5′ end) of the toehold region showed ~10-fold lower activity than C1. In the presence of 50 nM [H1] and 400 nM [H2], the catalytic activities (rate/[catalyst]) of C1 and MutC1 were 0.35 min^{-1} and 0.03 min^{-1}, respectively.

comprising H1, H2 and RepF:RepR can be thought as a DNA circuit with signal-amplification capacity to detect the presence of C1. Considering the extremely slow uncatalyzed reaction, the appreciable turnover rate of C1, and the ability to precisely measure the rates of catalysis enabled by real-time fluorescence readouts, we expected that very low concentrations of C1 could be detected using this circuit (Figure 4c). In fact, the presence of as low as 5 pM C1 could be unambiguously detected in our assays containing 50 nM H1, 400 nM H2 and 50 nM RepF:RepR complex within just a few hours (data not shown).

The detection of C1 by the circuit should be sequence-specific, since a mismatch in toehold or branch migration regions should in general impede toehold-mediated strand displacement by at least an order of magnitude (34,36,37). As expected, mutC1, which differs from C1 by just 1 nt, is 10-fold less active than C1 (Figure 4d).

The modularity of the design process (Figure 2) suggested that it should be possible to design a DNA circuit to detect virtually any single-stranded DNA input. However, redesigning the entire circuit each time is unnecessarily arduous. In addition, the amplification mechanism requires that the analyte DNA (in this case C1) essentially be structure-free, which poses a challenge for the detection of natural nucleic acids. Therefore, we wished to show that we could simply reuse the working circuit to detect various inputs, including structured nucleic acids, through the use of a transducer. We designed a molecular beacon-like molecule that could bind to a new nucleic acid sequence and in so doing create a toehold in the transducer that would mimic the catalytic activity of C1 (Figure 5a). The signal transducer (named hpC1) was generated by extending the 3′-end of C1 to form a hairpin loop where domain *1** of hpC1 is occluded by domain *1*. Therefore hpC1 should be catalytically inactive. The loop of hpC1 is complementary to the target nucleic acid. As in a molecular beacon (23,24), when the target nucleic acid is present, the loop should hybridize with the target, forming a rigid duplex and disrupting the stem formed by domain *1* and *1**. Even structured nucleic acid targets can be annealed to the loop of hpC1. The exposed domain *1** of hpC1 thereby serves as a toehold for initiating the amplification reaction. Similar molecular beacon-like transducers have also been used in the design of allosteric ribozymes (38,39) and deoxyribozymes (13,40).

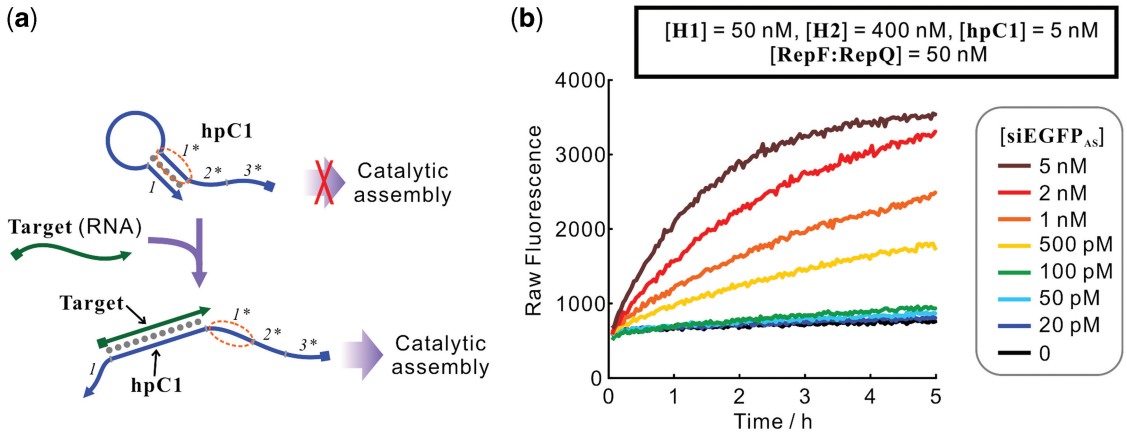

Figure 5. Detection of an RNA analyte. (**a**) Scheme of the molecular beacon-like signal transducer **hpC1**. (**b**) Performance of the signal transducer hpC1. Different concentrations of siEGFP$_{AS}$ were used as inputs for hpC1, followed by addition of H1, H2, and RepF:RepQ. The final concentration of each species is indicated in the panel.

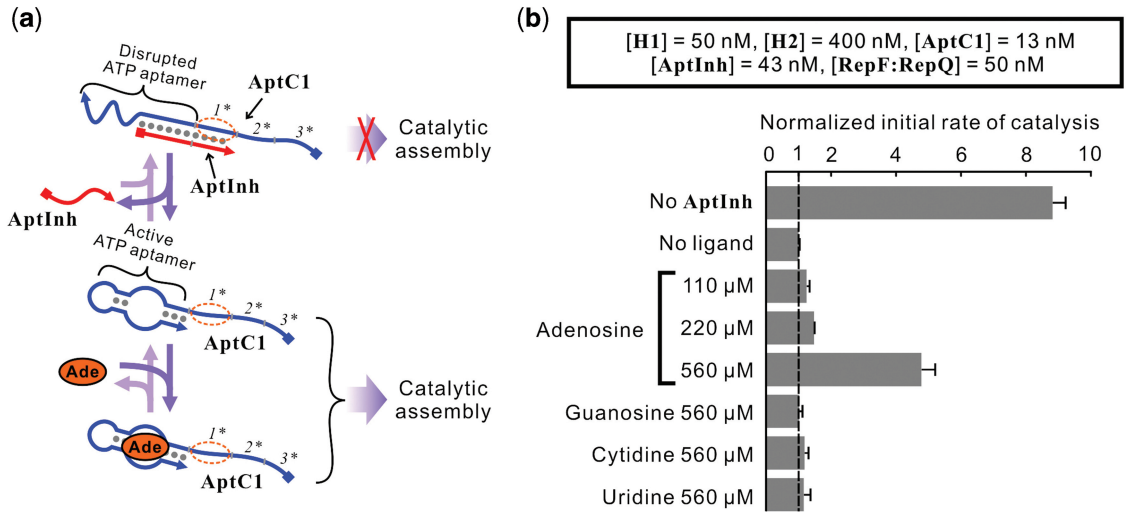

Figure 6. Detection of a small molecule analyte. (**a**) Scheme of the aptamer-based transducer that enables the circuit to detect adenosine. AptInh reversibly binds and inhibits the adenosine binding and hairpin assembly functions of AptC1. Adenosine shifts the equilibrium of binding and favors folded, catalytic AptC1. (**b**) Performance of the signal transducer. Different concentrations of adenosine and control nucleosides were incubated with the AptC1:AptInh complex (AptInh in excess), followed by the addition of H1, H2, and RepF:RepQ. The initial rates of catalysis were normalized to that of the reaction in which no nucleoside was added. In this reaction, the initial rate was 0.045 ± 0.01 nM min^{-1}, whereas the initial rate of the reaction in the absence of AptInh ('No AptInh') was 0.39 ± 0.02 nM min^{-1}. These two rates frame the dynamic range of this assay. The final concentration of each species is indicated in the panel.

Initially we chose the antisense strand of a siRNA directed against enhanced green fluorescent protein (named siEGFP$_{AS}$) as the nucleic-acid input. This RNA molecule is predicted [by mfold (41)] to fold into a hairpin structure with stability of −2.9 kcal/mol. As shown in Figure 5b, while 5 nM of hpC1 alone showed extremely low catalytic activity toward 50 nM H1 and 400 nM H2, the presence of the appropriate target RNA molecule substantially activated hpC1 in a dose-dependent manner. In the presence of 5 nM siEGFP$_{AS}$, hpC1 was activated by ~400-fold. The low background activity of hpC1 and the precise measurement of rates of catalysis allowed the detection of as little as 20 pM of siEGFP$_{AS}$ (data not shown).

In principle, non-nucleic acid could also be employed as inputs, similar to the design of allosteric ribozymes and deoxyribozymes (26,42). In particular, Wieland *et al.* (43) have recently shown that through the use of structure-switching aptamers, catalyzed hairpin assembly can be controlled by small molecule inputs, although these authors did not quantify the extent of amplification. We wished to similarly show that aptamers could be used in conjugation with our circuit for the detection of non-nucleic-acid analytes. To this end, we created an aptamer beacon in which an anti-adenosine aptamer (44), AptC1, was inhibited by a complementary strand, AptInh (Figure 6a). AptC1 also contained the necessary information (C1) to initiate the amplification reaction, and

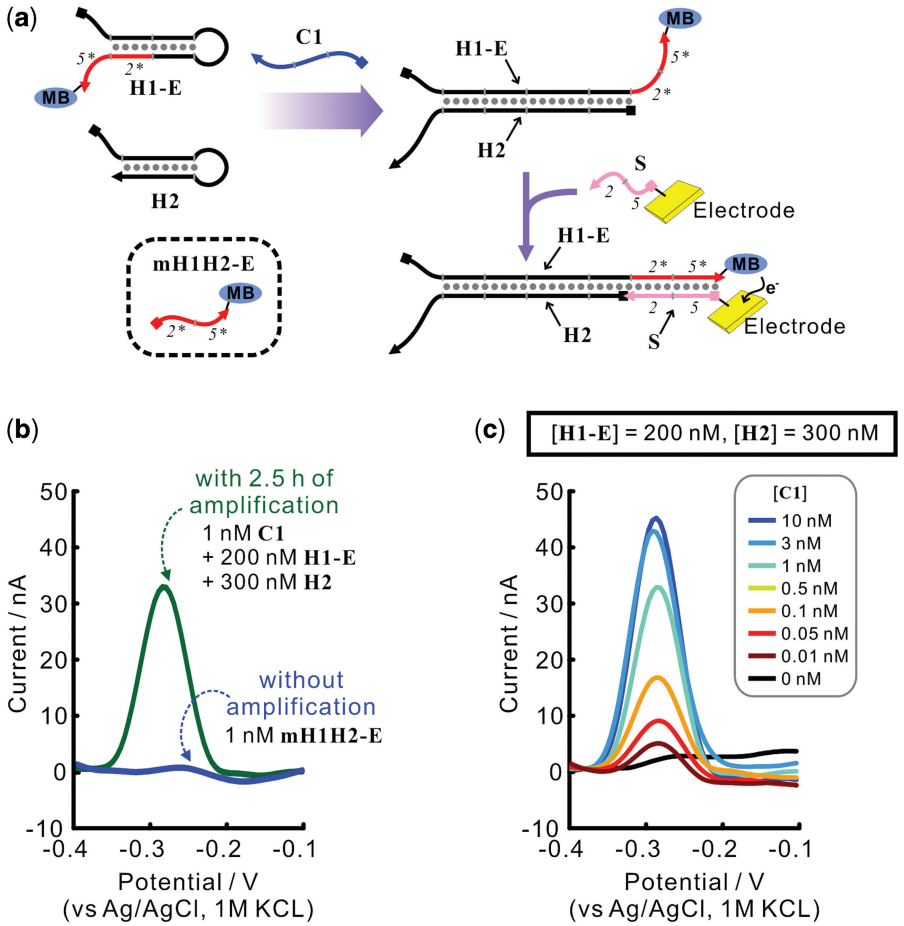

Figure 7. Electrochemical readout of the circuit. (**a**) Scheme of the electrochemical readout. The domain *6** of **H1** was truncated and the 3′ terminus of the truncated H1 was modified with a methylene blue (MB) moiety, to make H1-E. The H1-E:H2 complex (but not H1-E alone) can stably bind the surface of an electrode modified with strand **S**, leading to the detection of MB. (**b**) The amplification effect of the circuit, shown by the comparison between the MB-derived electrochemical (SWV) signal elicited by 1 nM mH1H2-E (blue line), and that elicited by 1 nM **C1** along with the circuit. (**c**) The electrochemical (SWV) signal elicited by different concentrations of **C1** with the circuit.

AptInh was also complementary to part of C1. When AptC1 is bound by AptInh it can neither bind its ligand nor catalyze the hybridization of H1 and H2. In contrast, free AptC1 can do both. As a result, when the ligand (in this case, adenosine) binds to and stabilizes AptC1 it shifts the equilibrium such that the duplex with AptInh is destabilized and the single-stranded toehold is available to activate the amplification reaction. We first observed that the 51-nt long AptC1 is an efficient catalyst (Figure 6b, sample 'No AptInh'), which is consistent with previous findings (45) that appending sequences to the catalyst of an enzyme-free DNA circuit does not qualitatively affect the efficiency of the catalyst, as long as the appended sequences do not form secondary structures that block the catalyst region. Next, as shown in Figure 6b, in the absence of adenosine, a combination of 13 nM AptC1 and 42 nM AptInh exhibited relatively low activity, whereas the presence of adenosine activated AptC1 in a dose-dependent manner. For example, in the presence of 110, 220 and 560 μM adenosine the catalytic activity of AptC1 was activated by 1.2-, 1.5- and 4.8-fold, respectively, whereas 560 μM guanosine, cytidine or uridine did not activate AptC1. The sensitivity and signal-to-background ratio can be systematically tuned by adjusting the length, sequence, and concentration of AptC1 (27), in accordance with the theoretical framework we developed previously (42).

Multimodal detection of analytes

An amplifier circuit would be most useful if it could be shown to be compatible with multiple analytical readouts. Having already shown compatibility with fluorescence sensing, we next asked whether the circuit could be readily adapted to an electrochemical readout. Domain *6** from H1 was truncated, and the 3′-end of the truncated H1 was then labeled with a methylene blue (MB) (28,29) moiety to form H1-E (Figure 7a). At the same time, a 16-nt capture oligonucleotide (named S) that was complementary to domains *2**–*5** (red in Figure 7a) of H1-E was conjugated to a gold electrode. The rationale was that H1-E can only transiently bind S (via 8 bp), whereas a H1-E:H2 complex could stably bind S (via 16 bp). Once H1-E:H2 was more strongly bound to S, the MB moiety

should be brought closer to the electrode over a great period of time, and this change could be detected via electrochemical methods such as square wave voltammetry (SWV).

We first proofed pieces of the electrochemical readout platform. The difference between 8-bp transient binding and 16-bp stable binding was first verified using fluorescent probes (Supplementary Figure S1). It should be noted that the absolute limit-of-detection (LOD) is highly dependent on assay conditions and devices. Therefore, direct comparisons of LODs between different experimental set-ups can be very misleading, especially when the purpose is to evaluate the amplifier. To estimate the potential level of signal amplification, we used a short MB-labeled oligonucleotide (mH1H2-MB, inset of Figure 7a) to mimic the amplification product H1-E:H2.

To test the performance of the amplifier, 200 nM H1-E and 300 nM H2 were mixed for 1 h in the presence of different concentration of C1. Then the reaction mixtures (15 μl) were added to the electrode modified with strand S (see Supplementary Figure S2 for electrode characterization) and incubated for another 1.5 h before SWV measurement. In a parallel experiment, 15 μl aliquots of mH1H2-MB at various concentrations were added to the electrode. As shown in Figure 7b, 1 nM mH1H2-MB did not elicit an observable current due to MB oxidation, whereas 1 nM of C1, through the DNA circuit, elicited an obvious MB oxidation peak at ~–0.28 V (versus Ag/AgCl, 1 M KCl). This signal was nearly half of the signal generated by 200 nM of mH1H2-MB (non-saturating, Supplementary Figure S3), which suggests a roughly 100-fold amplification by the amplifier circuit over the course of 2.5 h. The peak height and area were both positively correlated with the concentration of C1, and as low as 10 pM C1 could be detected using this method (Figure 7c).

As a second demonstration of the adaptability of the amplifier circuit, we attempted to facilitate the colorimetric detection of nucleic acid inputs, an urgent need for equipment-free, point-of-care diagnostics (46,47). Unfortunately, such methods usually suffer from low sensitivity, due in part to the lack of adequate signal amplification. While some signal amplification can be obtained via enzymatic turnover [such as the deoxyribozyme/ABTS reporter system (30–33)] it should be possible to further couple enzymatic turnover to the amplifier circuit, providing an additional level of signal generation. The quadruplex deoxyribozyme peroxidase that had previously been utilized was fused to domains 6-5-2. This reporter, Dz, was then inactivated by a complementary inhibitor strand, DzInh (Figure 8a). This approach is similar to that previously used for adaptation of the anti-adenosine aptamer to the input portion of the amplifier circuit, demonstrating the general ease with which these circuits can be modularly engineered. The H1:H2 complex can displace DzInh from Dz through toehold-mediated strand displacement and this will in turn allow the DNAzyme to fold into its active conformation.

To test this design, we incubated 600 nM of H1 and 900 nM of H2 with various concentrations of C1 for 4 h followed by the addition of Dz:DzInh complex, hemin, ABTS, and H_2O_2. Again, we used a short oligonucleotide (mH1H2, inset of Figure 8a) to mimic the amplification product H1:H2, and different concentrations of mH1H2 were added to the Dz:DzInh complex, hemin, ABTS and H_2O_2. As shown in Supplementary Figure S4 and Figure 8b, when peroxidase activity was assayed on a spectrophotometer, concentrations of mH1H2 <50 nM did not elicit detectable signal, whereas 1 nM of C1, through the circuit, elicited discernable signal, indicating a roughly 50-fold amplification of the input. Peroxidase activity was positively correlated with the concentration of C1. Moreover, 1–5 nM C1 produced sufficient peroxidase activity to cause a marked, visible color change that could be readily detected by eye (Figure 8c). In contrast, even 50 nM mH1H2 did not yield such a visible color change.

DISCUSSION

Adapting the amplification circuit to analytical applications

DNA circuits provide interesting opportunities for diagnostic applications. However, in order to function in assays the circuits must be engineered to take into account a number of practical considerations. While HCR and entropy-driven catalysis have begun to be characterized (45) and used in molecular detection applications (20,21), little was previously known about the efficiency, robustness, and application potential of catalyzed hairpin assembly.

Fortunately, since catalyzed hairpin assembly is based on DNA hybridization, secondary structure formation, and branch migration, a basic understanding of these processes also allows us to rationally design effective circuits. For example, since we envisioned executing the circuit as part of a point-of-care detection system where nuclease contamination is likely to be present, we decided not to include Mg^{2+} in the reaction buffer, as most nucleases required magnesium or another divalent ion for function. In consequence, DNA hybridization was weaker in our buffer than in buffers typically used in previous DNA circuits [(15,18,34,45,48); reactions at ~10 mM Mg^{2+}]. For this reason, we chose 8 nt as the length of the toehold, longer than toeholds previously used (typically 6–7 nt). The absence of Mg^{2+} should also disfavor non-specific reactions, which might have contributed to the more than 200-fold lower background reactivity of our circuit.

The elimination of 'clamp' domains greatly simplified the design process (Figure 2), since the overall length of designed sequences was reduced from 75–100 nt to 40–60 nt (even as the toehold length was increased to 8 nt). Moreover, oligonucleotides with such lengths can be faithfully synthesized as one piece, eliminating the necessity of preparing hairpins by enzymatic ligation of two shorter oligonucleotides (19). Simple denaturing PAGE purification of directly synthesized hairpins proved sufficient to achieve near-zero background with our designs. This modest methodological improvement will greatly reduce the turnaround time for designing and testing

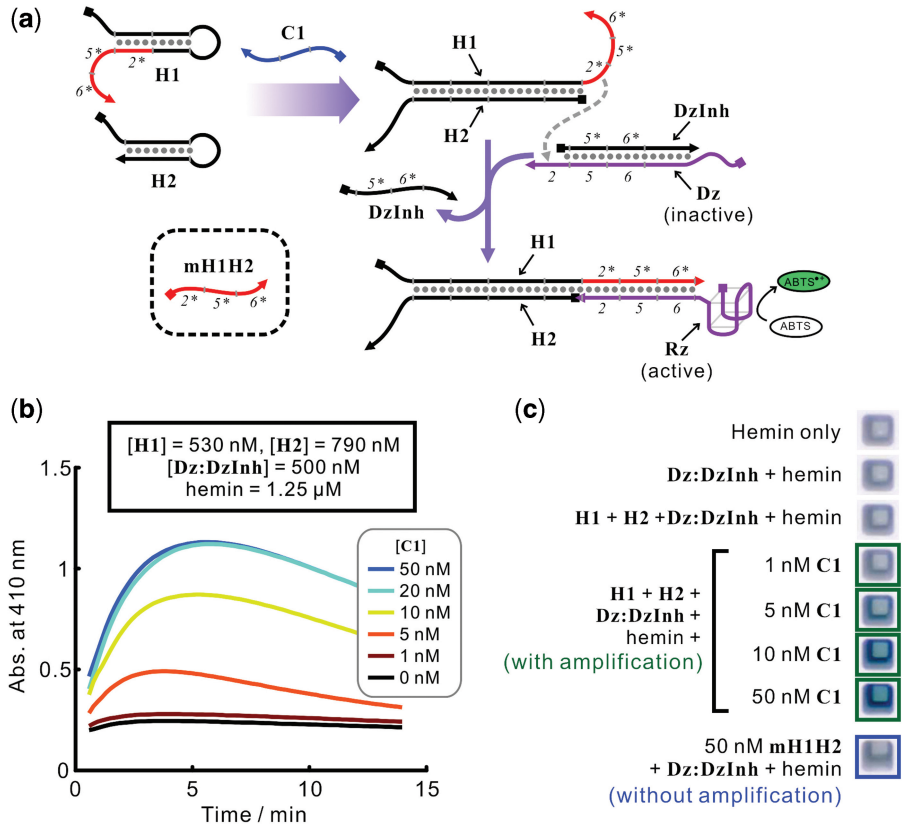

Figure 8. Colorimetric readout of the circuit. (**a**) Scheme of the colorimetric readout. The colorimetric reporter is made by the hybridization of Dz and DzInh. H1:H2 can displace DzInh from Dz, allowing the DNAzyme portion of **Dz** to fold into an active conformation and thereby catalyze the conversion of the colorless substrate ABTS to the green product $ABTS^{\bullet+}$ in the presence of hemin and H_2O_2. (**b**) Kinetics of formation of $ABTS^{\bullet+}$. All concentrations are listed as they were before the addition of hemin and H_2O_2. (**c**) The amplification effect of the circuit, shown by the comparison between the colorimetric signal elicited by 50 nM mH1H2 (the well with a blue outline), and that elicited by 1–50 nM C1 with the circuit (the wells with a green outline).

DNA circuits, and thus should begin to make these technologies much more widely accessible.

Speed of catalysis, efficiency of amplification, and possibility for cascading

In our circuit, the k_{cat} of **C1** is $>1\,min^{-1}$, making it one of the fastest known DNA catalysts. The k_{cat} values of the widely used trans-acting DNAzymes 10–23, 8–17 and E6 are $3\,min^{-1}$ (49), $0.6\,min^{-1}$ (50) and $0.04\,min^{-1}$ (51), respectively. Although this comparison is purely numerical rather than mechanistic, the rate of reaction is the primary consideration when a catalyst is to be used as a signal-amplifier (52). Thus, catalyzed hairpin assembly is in fact an excellent contender when a catalytic, DNA-based amplification is being considered.

The relatively fast reaction yielded ~100-fold signal amplification within just a few hours, a value that moves enzyme-free, colorimetric detection methods much closer to point-of-care applications. As an example, without using spectroscopic equipments or enzyme-based signal amplification (31–33), the well-developed peroxidase DNAzyme/ABTS reporter usually requires sub-micromolar concentrations of analyte to achieve visible signals (53). The signal amplification provided by the DNA circuit allowed us to readily detect target nucleic acid in low nanomolar range (Figure 8c), marking a two orders of magnitude improvement in sensitivity. Further kinetic characterizations, especially using pre-steady state methods, may reveal the rate-limiting step and thereby direct the development of even faster DNA circuits.

The programmability of DNA allows the product of one amplification reaction to act as the template or activator of another amplification reaction in order to achieve higher-level signal amplification. This principle has been extensively exploited in enzyme-dependent DNA amplification schemes such as PCR, loop-mediated isothermal amplification (LAMP) (54), nucleic acid sequence based amplification (NASBA) (55) and invader squared assays (56) to achieve quadratic or exponential amplification of initial signal. Similarly, catalyzed hairpin assembly reactions can also be cascaded (19) (see Supplementary Figure S5 for an example) to achieve higher levels of amplification.

However, a great challenge in cascading amplifiers is the amplification of background (also known as circuit leakage): the downstream amplifier can pick up the signal generated by the upstream amplifier in the absence of the input. Therefore, it is worthwhile to

investigate the origin of circuit leakage and consider whether it can be eliminated. In toehold-mediated enzyme-free DNA circuits (such as the one described in this work) there are two major sources of circuit leakage: impurities and toehold-independent reactions. Using our circuit as an example, some sub-population of H1 may be mis-synthesized and/or mis-folded and can therefore react with H2 in the absence of C1. On the other hand, even if all molecules are perfectly synthesized and folded, it is still possible that the stem of hairpin H1 can 'breathe' (even at very low frequency and with very short duration), leaving part of domain 3* transiently unpaired and able to interact with domain 3 of H2, leading to consequent strand displacement reactions and ultimately to the formation of a fully extended H1:H2 duplex. When the kinetics of a single amplifier are observed, leakage induced by impurities usually results in a fast initial increase in product concentration, which stops increasing as impure molecules are used up. In contrast, leakage induced by toehold-independent reactions can lead to a slow but steady increase of product concentration until all the reactants are used up.

In general, leakage induced by impurity may be eliminated by better synthesis and folding protocols, or by purification methods where substrates (in this case, H1 and H2) are first incubated together in the absence of catalyst (C1), and then the unreacted substrates are separated from each other and the product [see (15) and (18) for examples]. In contrast, toehold-independent leakage can only be mitigated by better designs. In the circuit described here, although we observe a very low level of leakage induced by impurity (compare the black and red traces in Figure 3b) we did not observe toehold-independent leakage. This suggests that, with improved purification methods, our design strategy is capable of producing amplifiers with extremely low leakage, and that these amplifiers can be cascaded to achieve better signal amplification.

An additional source of false-positive signal is mis-triggering of the catalytic circuit by irrelevant DNA or RNA present in the sample, especially when clinical or environmental samples are used. Earlier studies on entropy-driven catalytic DNA circuits showed that the addition of total cellular RNA or random DNA did not result in observable mis-triggering (18,45). We have observed similar results with catalyzed hairpin assembly (data not shown). This robustness is likely due to the remarkably high sequence specificity of toehold-mediated strand displacement. In addition, unnatural nucleobases such as isoC and isoG (57) can be incorporated into these types of enzyme-free DNA circuits to further decreases the likelihood of spurious interaction between the circuits and irrelevant nucleic acids.

Fault-tolerant signal detection

The real-time kinetics of DNA circuits has been routinely monitored by fluorescent reporters similar to that shown in Figure 1a, in which the exposure of a toehold leads to toehold-mediated strand displacement and separation of the fluorophore-bearing strand and the quencher-bearing strand. A subtlety in the design of such reporters that is not commonly appreciated is where to place the fluorophore and quencher. In most DNA circuit-related works, the fluorophore is on the strand that is ultimately displaced, whereas the quencher is on the strand that accepts the invading strand ('design I' in Supplementary Figure S6a). The position of fluorophore and quencher can also obviously be swapped ('design II' in Supplementary Figure S6a).

In previous studies (58), we designed the reporter based on 'design I', and added the quencher-bearing strand in 1.2-fold excess to ensure quenching. This allowed us to qualitatively detect the product of the circuit, but decreased our ability to quantitate the product, since the excess quencher strand can bind both the substrate and the product of the circuit and thereby confound the interpretation of the kinetic data.

In contrast, in 'design II' the reporter strand, whether fluor or deoxyribozyme, was double-stranded at the conclusion of the reaction (Supplementary Figure S6). The free quencher-bearing strand could only interact with its complement to form the substrate of the strand-exchange reaction (Supplementary Figure S6a), and thus could be added in even greater (2-fold) excess, ensuring efficient quenching. The DNAzyme reporter was largely double-stranded, preventing misfolding (Supplementary Figure S6b). Avoiding mispairing and misfolding in the reporter strands should allows greater overall flexibility in sequence design.

Although one could argue that the designs I and II should have identical performance if the reporter duplex is pre-annealed and purified on a native polyacrylamide gel (15), design II reduces the purification steps required to create a functional circuit. As larger and larger circuits are designed (59) with a view towards diagnostic and other applications, fault-tolerant design principles that allow less rigorous purification while still maintaining optimum performance will be essential.

The advantages of circuit-based molecular detection

One focus in the field of biosensor development has been the engineering of 'smart molecules', such as allosteric ribozymes/DNAzymes, aptamer beacons, and FRET-based signaling proteins (60), that not only recognize target molecules but also transduce the molecular recognition to observable signals. However, it is usually difficult to integrate many functions into one molecule and also to fine-tune each function. Molecular circuitry offers an opportunity to distribute tasks to many molecules that work collaboratively in a circuit to achieve higher-level performance (Supplementary Figure S7). In addition to amplifiers, other DNA-based signal processors such as logic gates (13,15) and thresholding devices (59) can also be used in DNA circuits to integrate information and parallelize signal transduction. Because of the inherent modularity of signal transduction and integration in DNA circuits, general design principles can be applied separately to each of these components.

SUPPLEMENTARY DATA

Supplementary Data are available at NAR Online.

ACKNOWLEDGEMENTS

The authors thank the Electrochemical Center at UT-Austin and Ms. Xiaole Chen for electrochemical equipments, and Steven Chirieleison for help on processing of electrochemical data.

FUNDING

Funding for open access charge: National Institutes of General Medical Sciences (R01GM077040) and National Institutes of Allergy and Infectious Diseases (R01AI092839).

Conflict of interest statement. None declared.

REFERENCES

1. Adler,M., Wacker,R. and Niemeyer,C.M. (2008) Sensitivity by combination: immuno-PCR and related technologies. *Analyst*, **133**, 702–718.
2. Niemeyer,C.M., Adler,M. and Wacker,R. (2007) Detecting antigens by quantitative immuno-PCR. *Nat. Protoc.*, **2**, 1918–1930.
3. Zhao,W., Ali,M.M., Brook,M.A. and Li,Y. (2008) Rolling circle amplification: applications in nanotechnology and biodetection with functional nucleic acids. *Angew. Chem. Int. Ed. Engl.*, **47**, 6330–6337.
4. Cho,E.J., Yang,L., Levy,M. and Ellington,A.D. (2005) Using a deoxyribozyme ligase and rolling circle amplification to detect a non-nucleic acid analyte, ATP. *J. Am. Chem. Soc.*, **127**, 2022–2023.
5. Gullberg,M., Fredriksson,S., Taussig,M., Jarvius,J., Gustafsdottir,S. and Landegren,U. (2003) A sense of closeness: protein detection by proximity ligation. *Curr. Opin. Biotechnol.*, **14**, 82–86.
6. Pai,S., Ellington,A.D. and Levy,M. (2005) Proximity ligation assays with peptide conjugate 'burrs' for the sensitive detection of spores. *Nucleic Acids Res.*, **33**, e162.
7. Levy,M. and Ellington,A.D. (2003) Exponential growth by cross-catalytic cleavage of deoxyribozymogens. *Proc. Natl Acad. Sci. USA*, **100**, 6416–6421.
8. Wang,F., Elbaz,J., Teller,C. and Willner,I. (2011) Amplified detection of DNA through an autocatalytic and catabolic DNAzyme-mediated process. *Angew. Chem. Int. Ed. Engl.*, **50**, 295–299.
9. Lincoln,T.A. and Joyce,G.F. (2009) Self-sustained replication of an RNA enzyme. *Science*, **323**, 1229–1232.
10. Lam,B.J. and Joyce,G.F. (2009) Autocatalytic aptazymes enable ligand-dependent exponential amplification of RNA. *Nat. Biotechnol.*, **27**, 288–292.
11. Vaish,N.K., Jadhav,V.R., Kossen,K., Pasko,C., Andrews,L.E., McSwiggen,J.A., Polisky,B. and Seiwert,S.D. (2003) Zeptomole detection of a viral nucleic acid using a target-activated ribozyme. *RNA*, **9**, 1058–1072.
12. Zhang,D.Y. and Seelig,G. (2011) Dynamic DNA nanotechnology using strand-displacement reactions. *Nat. Chem.*, **3**, 103–113.
13. Stojanovic,M.N. and Stefanovic,D. (2003) A deoxyribozyme-based molecular automaton. *Nat. Biotechnol.*, **21**, 1069–1074.
14. Benenson,Y., Gil,B., Ben-Dor,U., Adar,R. and Shapiro,E. (2004) An autonomous molecular computer for logical control of gene expression. *Nature*, **429**, 423–429.
15. Seelig,G., Soloveichik,D., Zhang,D.Y. and Winfree,E. (2006) Enzyme-free nucleic acid logic circuits. *Science*, **314**, 1585–1588.
16. Dirks,R.M. and Pierce,N.A. (2004) Triggered amplification by hybridization chain reaction. *Proc Natl Acad. Sci. USA*, **101**, 15275–15278.
17. Choi,H.M., Chang,J.Y., Trinh le,A., Padilla,J.E., Fraser,S.E. and Pierce,N.A. (2010) Programmable in situ amplification for multiplexed imaging of mRNA expression. *Nat. Biotechnol.*, **28**, 1208–1212.
18. Zhang,D.Y., Turberfield,A.J., Yurke,B. and Winfree,E. (2007) Engineering entropy-driven reactions and networks catalyzed by DNA. *Science*, **318**, 1121–1125.
19. Yin,P., Choi,H.M., Calvert,C.R. and Pierce,N.A. (2008) Programming biomolecular self-assembly pathways. *Nature*, **451**, 318–322.
20. Lin,C., Nangreave,J.K., Li,Z., Liu,Y. and Yan,H. (2008) Signal amplification on a DNA-tile-based biosensor with enhanced sensitivity. *Nanomedicine*, **3**, 521–528.
21. Niu,S., Jiang,Y. and Zhang,S. (2010) Fluorescence detection for DNA using hybridization chain reaction with enzyme-amplification. *Chem. Commun.*, **46**, 3089–3091.
22. Eckhoff,G., Codrea,V., Ellington,D.A. and Chen,X. (2011) Beyond allostery: Catalytic regulation of a deoxyribozyme through an entropy-driven DNA amplifier. *J. Syst. Chem.*, **1**, 13.
23. Drake,T.J. and Tan,W. (2004) Molecular beacon DNA probes and their bioanalytical applications. *Appl. Spectrosc.*, **58**, 269A–280A.
24. Santangelo,P., Nitin,N. and Bao,G. (2006) Nanostructured probes for RNA detection in living cells. *Ann. Biomed. Eng.*, **34**, 39–50.
25. Lu,Y. and Liu,J. (2006) Functional DNA nanotechnology: emerging applications of DNAzymes and aptamers. *Curr. Opin. Biotechnol.*, **17**, 580–588.
26. Liu,J., Cao,Z. and Lu,Y. (2009) Functional nucleic acid sensors. *Chem. Rev.*, **109**, 1948–1998.
27. Nutiu,R. and Li,Y. (2003) Structure-switching signaling aptamers. *J. Am. Chem. Soc.*, **125**, 4771–4778.
28. Fan,C., Plaxco,K.W. and Heeger,A.J. (2003) Electrochemical interrogation of conformational changes as a reagentless method for the sequence-specific detection of DNA. *Proc. Natl Acad. Sci. USA*, **100**, 9134–9137.
29. Lubin,A.A. and Plaxco,K.W. (2010) Folding-based electrochemical biosensors: the case for responsive nucleic acid architectures. *Acc. Chem. Res.*, **43**, 496–505.
30. Travascio,P., Li,Y. and Sen,D. (1998) DNA-enhanced peroxidase activity of a DNA-aptamer-hemin complex. *Chem. Biol.*, **5**, 505–517.
31. Weizmann,Y., Beissenhirtz,M.K., Cheglakov,Z., Nowarski,R., Kotler,M. and Willner,I. (2006) A virus spotlighted by an autonomous DNA machine. *Angew. Chem. Int. Ed. Engl.*, **45**, 7384–7388.
32. Cheglakov,Z., Weizmann,Y., Beissenhirtz,M.K. and Willner,I. (2006) Ultrasensitive detection of DNA by the PCR-Induced generation of DNAzymes: the DNAzyme primer approach. *Chem. Commun.*, 3205–3207.
33. Darius,A.K., Ling,N.J. and Mahesh,U. (2010) Visual detection of DNA from salmonella and mycobacterium using split DNAzymes. *Mol. Biosyst.*, **6**, 792–794.
34. Zhang,D.Y. and Winfree,E. (2009) Control of DNA strand displacement kinetics using toehold exchange. *J. Am. Chem. Soc.*, **131**, 17303–17314.
35. Zadeh,J.N., Steenberg,C.D., Bois,J.S., Wolfe,B.R., Pierce,M.B., Khan,A.R., Dirks,R.M. and Pierce,N.A. (2011) NUPACK: Analysis and design of nucleic acid systems. *J. Comput. Chem.*, **32**, 170–173.
36. Panyutin,I.G. and Hsieh,P. (1993) Formation of a single base mismatch impedes spontaneous DNA branch migration. *J. Mol. Biol.*, **230**, 413–424.
37. Panyutin,I.G. and Hsieh,P. (1994) The kinetics of spontaneous DNA branch migration. *Proc. Natl Acad. Sci. USA*, **91**, 2021–2025.
38. Burke,D.H., Ozerova,N.D. and Nilsen-Hamilton,M. (2002) Allosteric hammerhead ribozyme TRAPs. *Biochemistry*, **41**, 6588–6594.

39. Penchovsky,R. and Breaker,R.R. (2005) Computational design and experimental validation of oligonucleotide-sensing allosteric ribozymes. *Nat. Biotechnol.*, **23**, 1424–1433.
40. Chen,X., Wang,Y., Liu,Q., Zhang,Z., Fan,C. and He,L. (2006) Construction of molecular logic gates with a DNA-cleaving deoxyribozyme. *Angew. Chem. Int. Ed. Engl.*, **45**, 1759–1762.
41. Zuker,M. (2003) Mfold web server for nucleic acid folding and hybridization prediction. *Nucleic Acids Res.*, **31**, 3406–3415.
42. Chen,X. and Ellington,A.D. (2009) Design principles for ligand-sensing, conformation-switching ribozymes. *PLoS Comput. Biol.*, **5**, e1000620.
43. Wieland,M., Benz,A., Haar,J., Halder,K. and Hartig,J.S. (2010) Small molecule-triggered assembly of DNA nanoarchitectures. *Chem. Commun.*, **46**, 1866–1868.
44. Huizenga,D.E. and Szostak,J.W. (1995) A DNA aptamer that binds adenosine and ATP. *Biochemistry*, **34**, 656–665.
45. Zhang,D.Y. and Winfree,E. (2010) Robustness and modularity properties of a non-covalent DNA catalytic reaction. *Nucleic Acids Res.*, **38**, 4182–4197.
46. Liu,J. and Lu,Y. (2003) A colorimetric lead biosensor using DNAzyme-directed assembly of gold nanoparticles. *J. Am. Chem. Soc.*, **125**, 6642–6643.
47. Liu,J. and Lu,Y. (2005) Fast colorimetric sensing of adenosine and cocaine based on a general sensor design involving aptamers and nanoparticles. *Angew. Chem. Int. Ed. Engl.*, **45**, 90–94.
48. Zhang,D.Y. and Winfree,E. (2008) Dynamic allosteric control of noncovalent DNA catalysis reactions. *J. Am. Chem. Soc.*, **130**, 13921–13926.
49. Santoro,S.W. and Joyce,G.F. (1997) A general purpose RNA-cleaving DNA enzyme. *Proc. Natl Acad. Sci. USA*, **94**, 4262–4266.
50. Bonaccio,M., Credali,A. and Peracchi,A. (2004) Kinetic and thermodynamic characterization of the RNA-cleaving 8-17 deoxyribozyme. *Nucleic Acids Res.*, **32**, 916–925.
51. Breaker,R.R. and Joyce,G.F. (1995) A DNA enzyme with Mg(2+)-dependent RNA phosphoesterase activity. *Chem. Biol.*, **2**, 655–660.
52. Gerasimova,Y.V., Cornett,E. and Kolpashchikov,D.M. (2010) RNA-cleaving deoxyribozyme sensor for nucleic acid analysis: the limit of detection. *Chembiochem*, **11**, 811–817, 729.
53. Kolpashchikov,D.M. (2008) Split DNA enzyme for visual single nucleotide polymorphism typing. *J. Am. Chem. Soc.*, **130**, 2934–2935.
54. Notomi,T., Okayama,H., Masubuchi,H., Yonekawa,T., Watanabe,K., Amino,N. and Hase,T. (2000) Loop-mediated isothermal amplification of DNA. *Nucleic Acids Res.*, **28**, E63.
55. Compton,J. (1991) Nucleic acid sequence-based amplification. *Nature*, **350**, 91–92.
56. Griffin,T.J., Hall,J.G., Prudent,J.R. and Smith,L.M. (1999) Direct genetic analysis by matrix-assisted laser desorption/ ionization mass spectrometry. *Proc. Natl Acad. Sci. USA*, **96**, 6301–6306.
57. Switzer,C.Y., Moroney,S.E. and Benner,S.A. (1993) Enzymatic recognition of the base pair between isocytidine and isoguanosine. *Biochemistry*, **32**, 10489–10496.
58. Eckhoff,G., Codrea,V., Ellington,A.D. and Chen,X. (2010) Beyond allostery: catalytic regulation of a deoxyribozyme through an entropy-driven DNA amplifier. *J. Syst. Chem.*, **1**, 13.
59. Qian,L. and Winfree,E. (2009) A simple DNA gate motif for synthesizing large-scale circuits. *Lect. Notes Comput. Sc.*, **5347**, 70–89.
60. Miyawaki,A., Llopis,J., Heim,R., McCaffery,J.M., Adams,J.A., Ikura,M. and Tsien,R.Y. (1997) Fluorescent indicators for Ca2+ based on green fluorescent proteins and calmodulin. *Nature*, **388**, 882–887.